www.sciencemag.org/content/349/6247/500/suppl/DC1

Supplementary Materials for

S-Nitrosylation links obesity-associated inflammation to endoplasmic reticulum stress

Ling Yang, Ediz S. Calay, Jason Fan, Alessandro Arduini, Ryan C. Kunz, Steven P. Gygi, Abdullah Yalcin, Suneng Fu, Gökhan S. Hotamisligil*

*Corresponding author. E-mail: ghotamis@hsph.harvard.edu

Published 31 July 2015, *Science* **349**, 500 (2015)
DOI: 10.1126/science.aaa0079

This PDF file includes

Materials and Methods

Cell culture and reagents*:* HEK293A and MEF cells were cultured in DMEM (Invitrogen) with 10% cosmic calf serum. 200 nM thapsigargin (Sigma) was used to induce ER stress. 10ng/mL TNFα (EMD) and 1mM N^G-monomethyl-L-arginine (NMMA (Cayman Chemical) were used where indicated. Primary hepatocytes were isolated from nonfasted 10-week-old lean (C57BL/6J), *ob/ob* (*45*), IRE1α-floxed (provided by Dr. Iwawaki, Gunma University, Japan), or iNOS-deficient mice (Jackson Labs, B6.129P2-NOS2t^{m1lou}/J) by collagenase type X (Wako, Japan) perfusion method (*46*). Cells were washed with hepatocyte wash medium (Invitrogen), purified by Percoll (GE) density gradient separation, and resuspended in medium 199 containing Earle's salts (Invitrogen) and 5% fetal bovine serum (FBS). Cells were then seeded on collagen-coated plates (Bio-Rad) at a final density of 3.5×10^4 cells/cm^2. After 4h, attached cells were cultured with medium 199 containing Earle's salts (Invitrogen) and 5% FBS. After incubation for 16h, cells were cultured in HepatoZYME-SF media (Invitrogen) and transduced with indicated adenoviruses or treated with the indicated reagents.

Plasmids and mutagenesis: sXBP1-HA and full length XBP1-Flag constructs were first produced by PCR-amplification from mouse spliced XBP1 (sXBP1) or mouse unspliced XBP1 (uXBP1) cDNAs with the indicated tags on the C-terminus. A second PCR was performed to generate attB-flanked DNA fragments, and attP-containing donor vectors to generate entry vectors using the Gateway system (Invitrogen). Mouse iNOS expression plasmid was acquired from ThermoScientific. The human IRE1α-flag construct was a gift from Dr. Ron Prywes (Columbia University, US). RNase inactive mutant K907A and

the SNO mutations in the RNase domain (C931A, C951A and C931A+C951A) were generated by site-directed mutagenesis using the GeneTailor™ Site-Directed Mutagenesis System (Invitrogen).

Adenovirus transduction: The shRNA to target iNOS was designed against mouse iNOS (sense: 5'-GCTGTAACAAAGGAAATAGAA-3'). The hairpin template oligonucleotides were synthesized by Integrated DNA Technologies followed by annealing and insertion into the adenoviral shuttle vector using the BLOCK-it adenoviral RNAi expression system (Invitrogen). Adenoviruses carrying mouse sXBP1, mouse uXBP1, wild-type human IRE1α, RNase-mutant IRE1α (IRE1-RD), and IRE1α with mutations in two target nitrosylation sites in the RNase domain (IRE1-M1+M2) were generated using the ViraPower™ adenoviral expression system (Invitrogen). Adenoviruses were amplified in HEK293A cells and purified by CsCl gradient centrifugation. The viruses were titered and transduced into the cells as previously described (*47*). Primary hepatocytes were transduced with indicated adenoviruses at a titer of 1×10^7 VP/mL.

Western blot analysis: Proteins were extracted from cells or tissues and subjected to SDS–polyacrylamide gel electrophoresis, as previously described (*48*). Membranes were incubated with anti-p-IRE1α (Novus NB100-2323, 1:1000 dilution), anti-XBP1 (Santa Cruz SC-7160 1:500 dilution), anti-p-JNK (Cell Signaling 4668, 1:1000 dilution), anti-CHOP (Santa Cruz SC-2895S, 1:1000 dilution), anti-GRP78 (Stressgen SPA-826, 1:1000 dilution), anti-FLAG (Sigma M2, 1:1000 dilution), anti-IRE1α (Cell Signaling 3294, 1:000 dilution), anti-Tubulin (Abcam ab21058 1:5000 dilution), anti-p-AKT (Santa Cruz

sc-7985-R, 1:1000 dilution), anti-p-IR (Calbiochem 407707, 1:1000 dilution), anti-AKT (Santa Cruz sc-8312, 1:1000 dilution), anti-IR (Santa Cruz SC-811, 1:1000 dilution), or streptavidin-HRP (GE RPN1051) antibodies overnight at 4^{o}C. The membranes were incubated with the secondary antibody conjugated with horseradish peroxidase (Amersham Biosciences), and visualized using the enhanced chemiluminescence system (Roche Diagnostics). Densitometric analysis of western blot images were done by using Quantity One Software (Bio-Rad).

Chromatin immunoprecipitation assay: ChIP assays were performed using the SimpleChIP enzymatic chromatin IP system (Cell Signaling). Briefly, the soluble chromatin derived from 1×10^{7} primary hepatocytes of 10-week-old *ob/ob* mice and their lean controls were used. Primers used to amplify XBP1 target promoter regions were purchased from SABiosciences (EpiTect ChIP qPCR Primers). Anti-XBP1 antibody was purchased from Santa Cruz. These experiments were performed with 4 mice per group.

Glutathione assay: Hepatic reduced glutathione (GSH) content was measured using a Glutathione assay system (Cayman Chemical). Briefly, 200mg liver tissue was homogenized and the samples were deproteinized by using the metaphosphoric acid and triethanolamine method. The GSH level was detected by using a colorimetric 96-well plate reader at 405nm. The total GSH levels were normalized to liver tissue weight.

Quantitative real-time RT-PCR: Total RNA was isolated using Trizol reagent (Invitrogen) and converted into cDNA using a cDNA synthesis kit (BioRad). Quantitative real-time RT-PCR analysis was performed using SYBR Green in a real-time PCR

apparatus (Applied Biosystems). The primers were synthesized and purchased from Integrated DNA Technologies.

Gene	Forward	Reverse
Mouse Blos1	CCCGCCTGCTCAAAGAACA	GAGGTGATCCACCAACGCTT
Mouse Col6a6	AGCCAGGAGGACCTAGATCAT	TCTTGTTGTTACCCGTGCTCA
Mouse Dnajb9	CCCCAGTGTCAAACTGTACCAG	AGCGTTTCCAATTTTCCATAAATT
Mouse EDEM	AAGCCCTCTGGAACTTGCG	AACCCAATGGCCTGTCTGG
Mouse Erdj4	CCCCAGTGTCAAACTGTACCAG	AGCGTTTCCAATTTTCCATAAATT
Mouse Ero1l	TCAGTGGACCAAGCATGATGA	TCCACATACTCAGCATCGGG
Mouse Galnt10	TTTTCTTGGGAGCTGAACAAAGG	CTGTGCGTCCCTCCTGATA
Mouse-GRP78	ACTTGGGGACCACCTATTCCT	ATCGCCAATCAGACGCTCC
Mouse HERP	CATGTACCTGCACCACGTCG	GAGGACCACCATCATCCGG
Mouse Hgsnat	CGGGCGGAGCCAGATTTAG	GCTCGTCCCCAAGAGTTCAT
Human IRE1	ACGAAACTTCCTTTTACCATCCC	CGATGACAAAGTCTGCTGCTT
Mouse Mgat2	CGGAAGGTGCTAATCCTGACG	CCGATTCGTTTGAGACCCTG
Mouse iNOS	GTTCTCAGCCCAACAATACAAGA	GTGGACGGGTCGATGTCAC
Mouse nNOS	CCCAACGTCATTTCTGTCCGT	CTGACCCGTTCCTTCACCAG
Mouse eNOS	TCAGCCATCACAGTGTTCCC	ATAGCCCGCATAGCGTATCAG
Mouse p58IPK	GGCGCTGAGTGTGGAGTAAAT	GCGTGAAACTGTGATAAGGCG
Mouse Pdia5	GACCCGCAATAACGTGCTG	CTCGGTCATACTGCATGTGAAA
Mouse Pdia3	GAGGCTTGCCCCTGAGTATG	GTTGGCAGTGCAATCCACC
Mouse PDI	CAAGATCAAGCCCCACCTGAT	AGTTCGCCCCAACCAGTACTT
Mouse Pdgfrb	TCCAGGAGTGATACCAGCTTT	CAGGAGCCATAACACGGACA
Mouse Pmp22	CATCGCGGTGCTAGTGTTG	GATCAGTCGTGTGTCCATTGC
Mouse Scara3	TGAAGACGAGGACATGCCATC	GAGGTACAAAATCCGCACTGA
Mouse Trim16	AGAGGTGGACCTTCGGTGTAT	CAGACTTATGGTTAGCTTGGAGC
Mouse sXBP	GGTCTGCTGAGTCCGCAGCAGG	AGGCTTGGTGTATACATGG
Mouse uXBP1 set1	ACGGCCTTGTGGTTGAGAAC	TGTCCATTCCCAAGCGTGTT
Mouse uXBP1 set2	AGCAGCAAGTGGTGGATTTG	GAGTTTTCTCCCGTAAAAGCTGA
Mouse uXBP1 set3	GACAGAGAGTCAAACTAACGTGG	GTCCAGCAGGCAAGAAGGT

In vitro splicing assay: The *in vitro* XBP1 splicing assays were performed as described by Lisbona *et al.* (*49*) with modifications. Briefly, IRE1α was immunoprecipitated from IRE1α-deficient MEFs reconstituted with FLAG-IRE1α from a 10cm tissue culture plate or from liver tissue lysates (total of 3 mg protein). The protein mix was then incubated

for 1 hr at 30°C with 15μg of total mRNA as substrate (obtained from mouse brain cortex to minimize basal XBP-1 mRNA splicing levels) in kinase buffer containing 20mM HEPES (pH 7.3), 1mM DTT, 10mM magnesium acetate, 50mM potassium acetate, and 2mM ATP. The mRNA was re-extracted with 500μl of Trizol, and sXBP1 was monitored and quantified using a PCR-based assay. Immunoprecipitation used IgG as a control.

Biotin switch assay: Biotin switch assays were performed as described by Snyder *et al.* (*20*) and Derakhshan *et al.* (*19*) with minor modifications. Briefly, cells (from two 10cm tissue culture dishes) or liver tissues were homogenized in HENS buffer (250mM HEPES, pH 7.7, 1mM EDTA, 0.1mM neocuproine, 0.4% CHAPS). Two mg protein was used to perform the experiments. Protein samples were blocked with MMTS buffer (25mM HEPES, pH 7.7, 0.1mM EDTA, 10μM neocuproine, 1% SDS, 20mM MMTS) and incubated at 50°C for 20 min with frequent vortexing. The MMTS was removed by protein precipitation with acetone. *S*-nitrosylated proteins were then modified with biotin (0.2mM biotin-HPDP, Pierce) in HPDP buffer (25mM HEPES, pH 7.7, 0.1mM EDTA, 1%SDS, 10μM Neocuproine, 10mM ascorbic acid sodium salt) for 1h at 2°C in the dark. Biotinylated proteins were purified with acetone, followed by pulling down using streptavidin-agarose (GE) in neutralization buffer (20mM HEPEs, 100mM NaCl, 1mM EDTA, 0.5% Triton X-100). The beads were washed with neutralization buffer with 600mM NaCl, and samples were eluted using an elution buffer (20mM HEPEs, 100mM NaCl, 1mM EDTA, 100mM 2-ME). Biotinylated proteins were detected by horseradish peroxidase (HRP)-conjugated streptavidin (Amersham), and the proteins of interest were examined with specific antibodies as indicated.

Structure generation of S-nitrosylated cysteine and normal mode analysis: The crystal structure of human IRE1α/ERN1 was downloaded from the Protein Data Bank (*50*) (PDB ID: 3P23). S-nitrosocysteine was generated with the molecular modeling "S-nitrosator" Python script available from the Timerghazin laboratory (*25*).

Biochemical assays for IRE1α:

In vitro RNase cleavage assay: Recombinant Human IRE1α (465-977) proteins (IRE1c) were purchased from Sino Biological Inc. (Beijing, China). 5′-Carboxyfluorescein (FAM)- and 3′-Black Hole Quencher (BHQ)-labeled XBP1 single stem-loop mini-substrate (5'FAM GAACAAGAUAUCCGCAGCAUAUACAGUUC3'BHQ) (*51*) and 5'-FAM and 3'-BHQ labeled SPARC single stem-loop mini-substrate (5'FAMGUGGGAGAGAUCCCUGCAGAACCCAC 3'IABFQ) were purchased from Biosearch Technology and IDT. RNA cleavage reactions were conducted at 30^{o}C in cleavage buffer containing 20mM HEPES (pH 7.0 at 30 μC), 70mM NaCl, 2mM ADP (pH 7.0), 2mMMgCl_2, 5mMDTT, 5% glycerol as described before (*34*). IRE1c was incubated with NO donors for 20 min in cleavage buffer at room temperature in the dark, followed by incubation with 3μM RNA XBP1 substrate for 45min or SPARC substrate for 15min at 30^{o}C. The reaction was quenched by adding urea to a final concentration of 4M, the cleavage products were resolved by 19% urea PAGE, and gels were scanned and band intensity quantified.

IRE1α substrate recognition assays*: UV cross-linking and immunoprecipitation assay (CLIP)* was performed as described before (*30*). Briefly, IRE1$\alpha^{-/-}$ MEFs were reconstituted with adenovirus-mediated IRE1-WT or IRE1-M1+2 variant, followed by

treatments with Tg in the absence or presence of TNFα. Cells then were washed with cold PBS and UV cross-linked at 200mj/cm^2, and the IRE1α complexes were immunoprecipitaed from 2 μg cell lysate with anti-IRE1α antibody (Cell Signaling). After Partial RNA and DNA digestion, RNAs were isolated from this protein-RNA complex using phenol/chloroform (Ambion), and the full length XBP1 abundance was detected by qRT-PCR. For *fluorescence polarization assay,* recombinant Human IRE1α peptide (aa465-977, IRE1c) was purchased from Sino Biological Inc (Beijing, China). 5'-Fluorescein labeled 2'-deoxy substitutions of HP21 RNA (FLdCdCdGdCdAdG) (32), 5'-Fluorescein labeled 2'-deoxy substitutions of RIDD RNA (Fl.A.A.A.A.A.U.dG.dC.A.A.A.A.A), and the non-labeled oligos were ordered from Thermo Scientific. The fluorescence polarization assay was performed as described in a previous study (*52*). Briefly, IRE1c (500nM) was prepared in cleavage buffer, and increasing concentrations of IRE1c were incubated with DMSO, SNAP or GSNO for 20min at room temperature in the dark. The fluorescein labeled RNase-resistant RNA analogs (1μM) were added to the proteins in the absence or presence non-labeled competitors for 15min at 30^{o}C, the results were read by measuring using Spectra M5 plate reader. The results were normalized by setting the reactions without IRE1c to 0.

IRE1α oligomerization assay: Oligomerization assay was adapted from a previously published protocol (*42*). Briefly, increasing concentrations of IRE1c were incubated with DMSO, SNAP (5mM) or GSNO (0.25mM) for 20min at room temperature in the dark. The samples were then added with Native sample buffer (Bio-Rad), resolved in 8% Native-PAGE, and immunoblotted for IRE1α.

Mouse models and administration of the adenoviruses: Animal care and experimental procedures were performed with approval from animal care and use committees of Harvard University. Male *ob/ob* mice and wild type lean controls at 6 weeks of age were purchased from Jackson Labs, kept on a 12-hr light cycle, and fed with regular diet for 4-8 weeks. Mice used in the diet-induced obesity model were male C57BL/6J purchased from Jackson Labs, and placed on HFD (35.5% fat, 20% protein, 32.7% carbohydrates, Research Diets) immediately after weaning at 3-weeks of age. The IRE1α conditional deletion model was kindly provided by Dr. Takao Iwawaki (Riken, Japan). Adenoviruses carrying GFP, shiNOS, LacZ-shRNA, Cre, sXBP1, uXBP1, IRE1α, IRE1-RD, or IRE1-M1+2 were delivered into *ob/ob* mice, lean controls, or IRE1α-flox mice via injection at a titer of 5×10^9 ifu/mouse. In co-expression experiments, two types of viruses were first mixed with equal titers, and each virus was delivered at a final concentration of 2.5×10^9 ifu/mouse. After 7-10 days, glucose and insulin tolerance tests, and insulin injections were performed as described below. Tunicamycin was intraperitoneally administrated to *ob/ob* mice at 0.5mg/kg in 150mM dextrose. After 6hrs, tissues were harvested, frozen in liquid nitrogen, and kept at -80°C until processing.

Glucose, insulin tolerance tests and insulin infusions: Glucose tolerance tests were performed by intraperitoneal glucose injection ($1\ g \cdot kg^{-1}$) after an overnight fast. Insulin tolerance tests were performed by intraperitoneal insulin injection ($1.0\ IU \cdot kg^{-1}$) after 6hrs day time food withdrawal (*48*). Insulin infusion studies were performed with the *ob/ob* mice with 6 hrs day-time food withdrawal. Briefly, *ob/ob* mice were anaesthetized with an intraperitoneal injection of 100mg/kg ketamine and 10mg/kg xylazine, and insulin ($0.75\ IU \cdot kg^{-1}$) or phosphate buffered saline (PBS) was infused into the portal vein in a

200µl volume. Three minutes after infusion, tissues were removed, frozen in liquid nitrogen and kept at -80 °C until processing.

S-Nitrosylation of synthetic peptides: Two peptides (Peptide1 sequence: KLPDDFV**C**YFTSRK, Peptide2 sequence: KYRAMEL**C**SHERLK) derived from the RNase domain of huam IRE1α were synthesized and purchased from Thermo Scientific. The MS analysis was performed as described by Wang *et al*. (*53*) with modifications. Briefly, each peptide was mixed to a final concentration of 200 pmol/µL with a 10-fold molar excess of GSNO (Calbiochem) in solution containing 1mM EDTA and 0.1mM neocuproine (pH 7.4). The reaction was carried out at 37^{o}C in the dark, and resulting peptides solution were quenched by diluting the reaction mixture 1:20 in 50% acetonitrile + 1% formic acid. The quenched reaction was analyzed by direct infusion into an Exactive Orbitrap mass spectrometer with the following settings: Ion time, 1000ms; Resolution, 50,000; AGC Target 1e^{6}.

Statistical analysis: The results are expressed as means±standard error of the mean; *n* represents the number of individual experiments. Statistical analysis was performed by Student's *t*-test, multiple t tests followed by Holm-Šídák method, or One-way ANOVA followed by post-hoc Tukey's test, or two-way ANOVA followed by post-hoc Bonferroni test, using Prism as indicated in the figure legends.

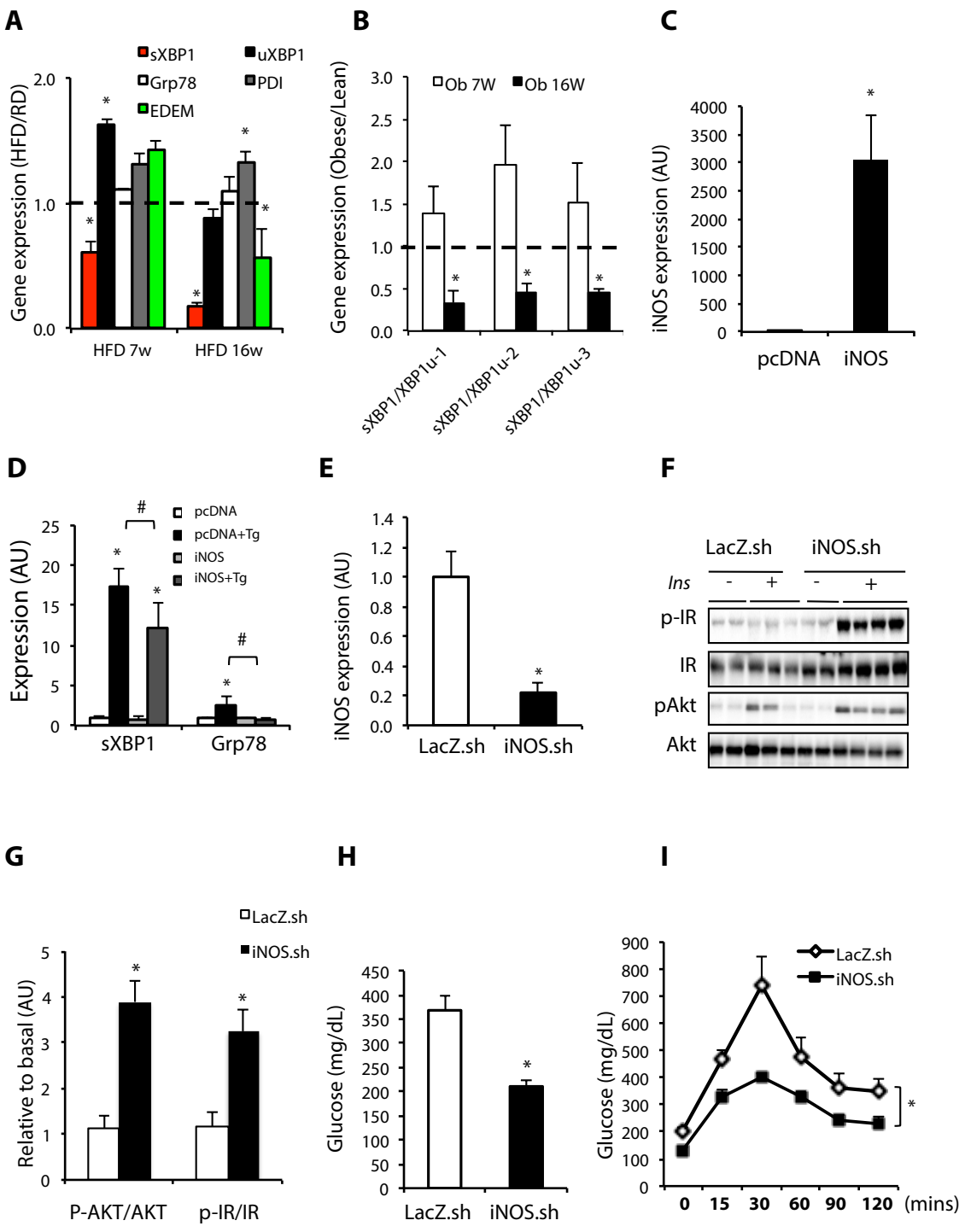

Supplemental Figure 1

Figure S1. Obesity-associated chronic inflammation and increased iNOS activity contributes to decreased sXBP1 in liver. A. Expression of UPR modulators in the livers of 7- and 16-week high fat diet (HFD)-fedmice relative to lean controls (dashed line indicates lean level). * indicates statistical significance between lean and obese mice (multiple *t* tests) and significance was determined by Holm-Šídák method using Prism, n=4. Data are representative of two individual sets of mice. **B.** Ratio of sXBP1 to uXBP1 gene expression in the livers from *ob/ob* mice and lean controls at different ages were examined by qRT-PCR, using different primers. * indicates statistical significance between lean and obese mice by Student's *t*-test (*p<0.05), n=4. **C.** Quantitative RT-PCR for iNOS expression in primary hepatocytes isolated from iNOS-deficient mice, and reconstituted with iNOS or control plasmid (pcDNA). Data are presented as relative gene expression levels normalized to controls (pcDNA). * indicate statistical significance determined by Student's *t*-test (p<0.05), n=4. **D.** mRNAs coding for sXBP1 and Grp78 in primary hepatocytes from $iNOS^{-/-}$ mice reconstituted with iNOS or control plasmid (pcDNA) in the presence or absence of thapsigargin (Tg). Results are presented in each group normalized to controls (pcDNA). Data are presented as mean ± S.E.M. Asterisk indicates statistical significance compared with control, and # indicates statistically significant differences between treatments (one-way ANOVA followed by post-hoc Tukey's test), n=3. **E.** Quantitative RT-PCR analysis of iNOS mRNA expression level in livers from *ob/ob* mice with iNOS suppression (iNOS.sh) and controls (LacZ.sh). Data are presented as relative gene expression levels normalized to controls. Data are presented as mean ± S.E.M. and * indicates statistical significance determined by Student's *t*-test (p<0.05), n=6. **F.** Hepatic insulin action in *ob/ob* mice with iNOS suppression. Ins: insulin. The densitometric analysis is shown in (**G**). **H.** Glucose levels were measured in mice with iNOS suppression (iNOS.sh) and controls after 6hr food withdrawal. * indicates statistical significance between LacZ.sh and iNOS.sh mice by Student's *t*-test (*p<0.05), n=7-9. **I.** Glucose tolerance tests in *ob/ob* mice transduced with Ad-shiNOS (iNOS.sh) or control. * indicates statistical significance following two way ANOVA analysis. All data are presented as mean±S.E.M., n=7-9. Data is representative of two independent cohorts of mice.

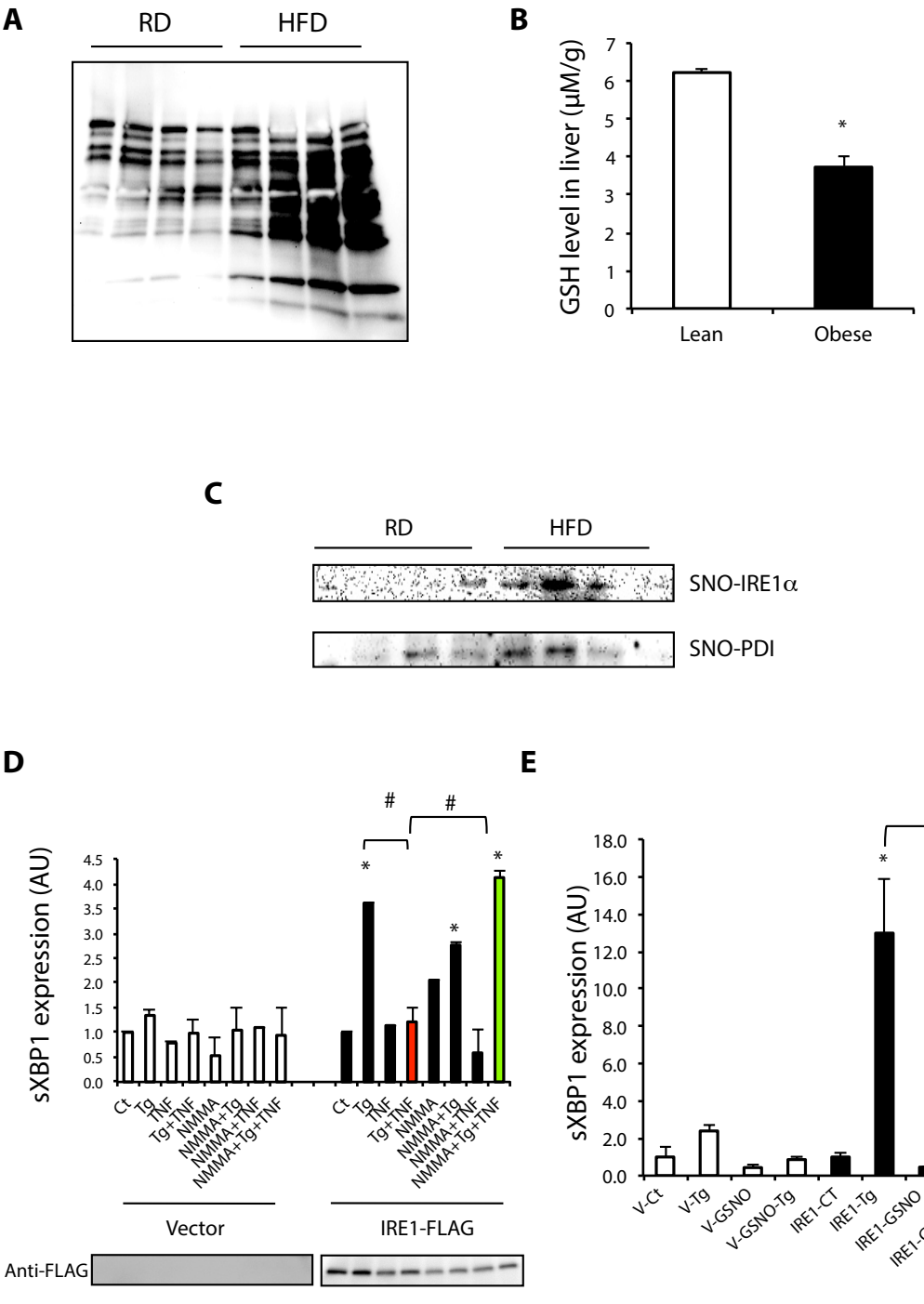

Supplemental Figure 2A-E

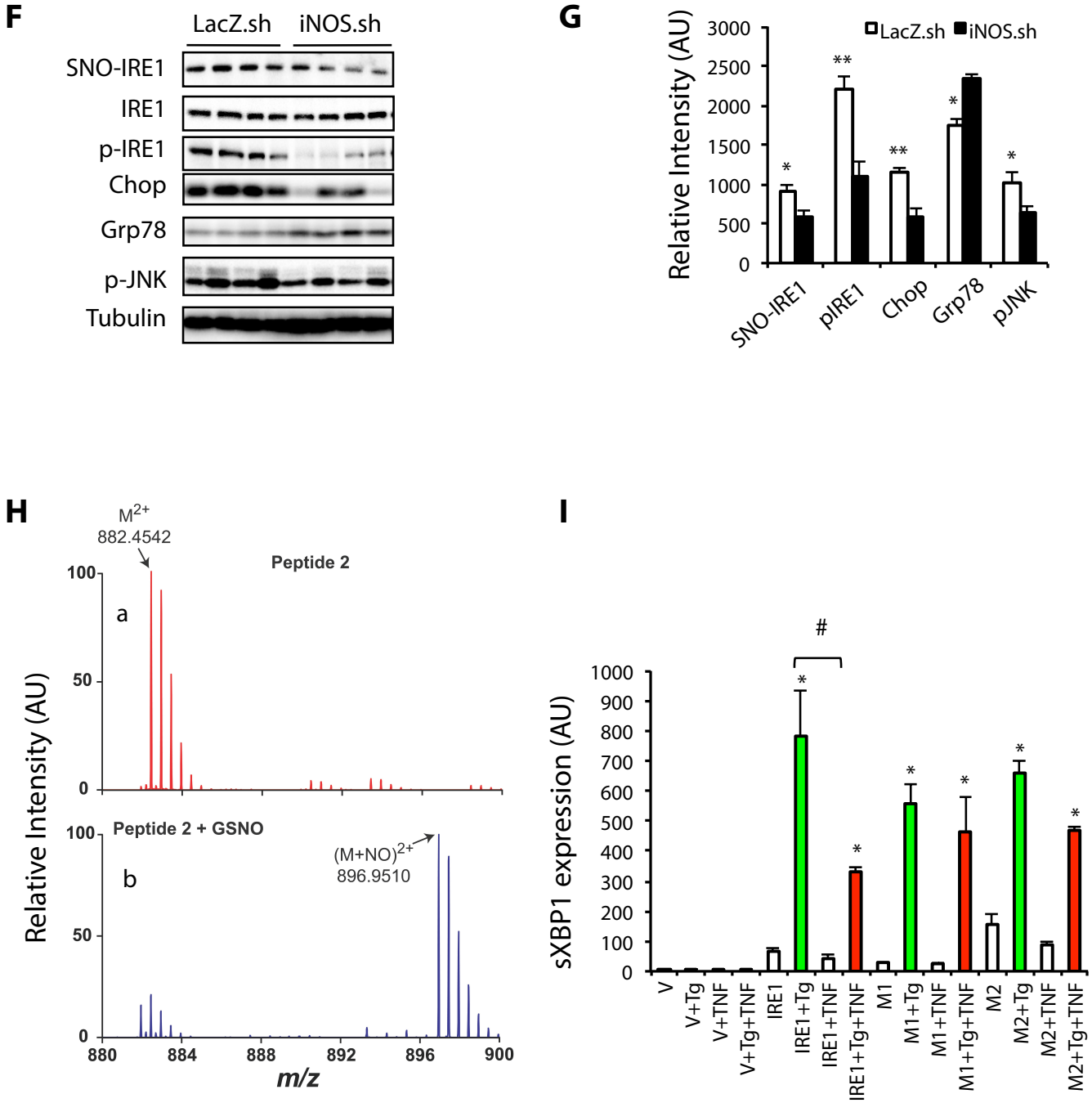

Supplemental Figure 2F-I

Figure S2. Regulation of general hepatic nitrosylation in obesity and reduction of IRE1α RNase activity. A. Profile of hepatic s-nitrosylated proteins in HFD-fed and age-matched regular diet (RD)-fed mice. Data are representative of two individual cohorts of mice. **B.** Hepatic GSH content was measured in *ob/ob* mice (obese) and lean controls. Data are presented as mean±S.E.M. Asterisk indicates statistical significance determined by Student's *t*-test (*$p<0.05$), n=3. **C.** S-nitrosylation of IRE1α or PDI was examined by biotin switch method followed by western blot analysis in livers of mice fed with HFD or RD. Data is representative of two individual sets of mice. **D.** sXBP1 mRNA was examined by quantitative RT-PCR (qPCR) in IRE1α$^{-/-}$ MEFs reconstituted with FLAG-IRE1α or control plasmids (vector). Results are presented values in treated samples normalized to basal levels in each group. IRE1α expression was examined by western blot analysis and shown in the panel below. NMMA, an iNOS inhibitor; Tg: thapsigargin, n=3. **E.** MEFs were transfected with FLAG-IRE1α or control plasmid (V), followed by treatment with thapsigargin in the presence or absence of GSNO, a chemical NO donor, and qPCR was performed to examine sXBP1 mRNA. Asterisk indicates statistical significance compared to control, and # indicates statistically significant differences between group (one-way ANOVA followed by post-hoc Tukey's test), n=3. **F.** S-Nitrosylation of IRE1α (SNO-IRE1α) and UPR status in livers of *ob/ob* mice following iNOS suppression. **G.** Densitometry analysis of blots in (E). Asterisks indicate statistical difference (Student's *t*-test) compared to control, * $p<0.05$, ** $p<0.01$. **H.** MS analysis of S-nitrosylated peptide 2, which includes C951 in the RNase domain of human IRE1α. Top: MS spectrum of unmodified peptide 2, double-charged M^{2+} (*m/z* 882.4542). Bottom: MS spectrum of peptide 2 after GSNO modification $(M+NO)^{2+}$ (*m/z* 896.9510). Nitrosylation of this peptide results in a *m/z* change of +14.4968 in the double-charged state. **I.** Quantitative RT-PCR for sXBP1 expression in IRE1α$^{-/-}$ MEFs reconstituted with wild type IRE1α (IRE1), IRE1α with mutations in two potential SNO sites in the RNase domain (M1:C931A, M2:C951A), or control plasmid (V). Results are presented as gene expression level in each group normalized to controls. All data are shown as mean±S.E.M., asterisk indicates statistical significance compared with control, and # indicates statistically significant differences between treatments (one-way ANOVA followed by post-hoc Tukey's test, n=3).

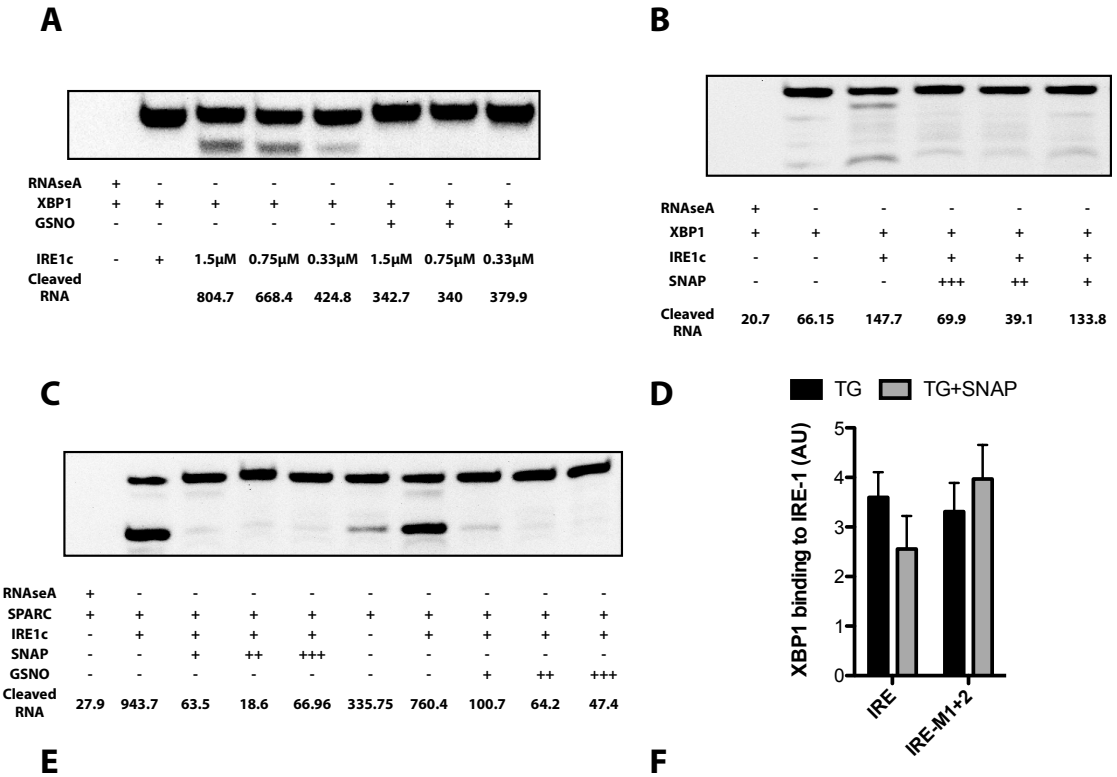

Supplemental Figure 3

Figure S3. The effect of IRE1α S-nitrosylation on RNase enzyme activity, XBP1 binding, and formation of protein complexes. A. Urea PAGE of sXBP1 substrate (labeled with FAM at the 5″ end) cleavage by different dose of IRE1c in the absence or presence of the chemical NO donor, GSNO (0.25mM). RNase A was used as a control. The quantification of cleaved RNA is shown as band intensity ($INTmm^2$). Data are representative of two individual experiments. **B.** Urea PAGE of sXBP1 substrate cleavage by IRE1c in the absence or presence of different doses of SNAP. The quantification of cleaved RNA is shown as band intensity ($INTmm^2$). **C.** Urea PAGE of RIDD substrate (SPARC, labeled with FAM at the 5′ end) cleavage by IRE1c in the absence or presence of chemical NO donors, SNAP (5mM) or GSNO (0.25mM). The quantification of cleaved RNA is shown as band intensity ($INTmm^2$). Data are representative of two individual experiments. **D.** The interaction between IRE1α and unspliced XBP1 was examined by CLIP assay in IRE1α$^{-/-}$ MEFs reconstituted with wild type IRE1α or IRE1-M1+2. TG, Thapsigargin (200nM, 2hrs). Data are shown as mean±S.E.M. Data are representative of three individual experiments. **E.** Binding of a RNase-resistant RIDD RNA analog with IRE1c in the absence or presence of NO donor was analyzed by fluorescence polarization assay using a nonfluorescent RIDD as a competitor. The data are presented as units of millipolarization (mP), and the Ki is showed in the bottom panel. Data are representative of three individual experiments. **F.** IRE1α$^{-/-}$ MEFs were reconstituted with FLAG-IRE1α, and the cells were treated with thapsigargin (TG) in the presence or absence of TNFα. Immunoprecipitation was performed by using anti-FLAG antibody followed by western blot analysis. **G**. Summary of the approaches performed to explore the effect of S-nitrosylation on IRE1α and its RNAse activity.

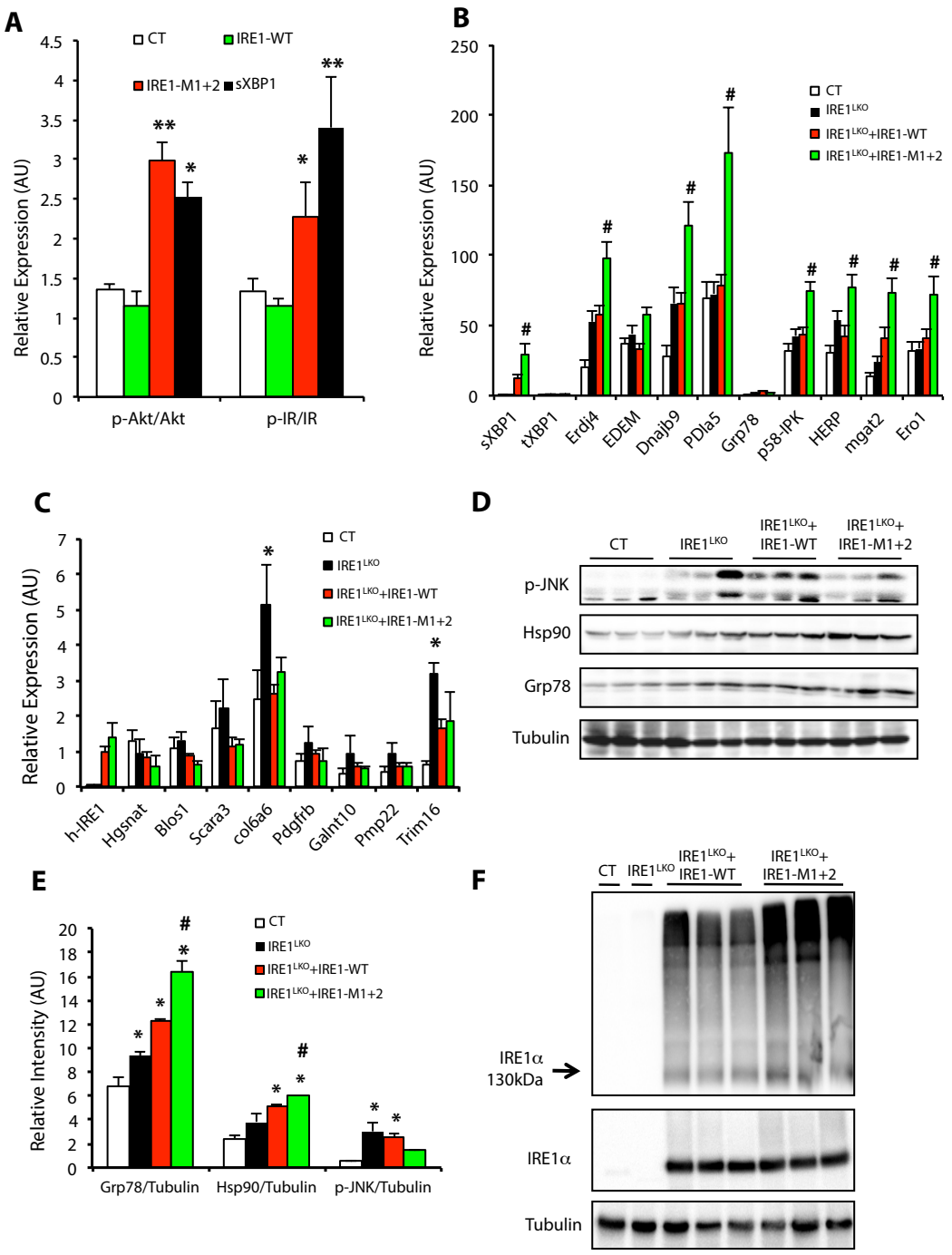

Supplemental Figure 4

Figure S4. Molecular and biochemical outcomes of S-nitrosylation of IRE1α *in vivo*. A. Densitometric analysis of western blots shown Figure 4B, derived from *ob/ob* mice transduced with adenovirus containing sXBP1, wild type IRE1α or nitrosylation resistant IRE1-M1+2. Asterisk indicates statistical significance compared with control (one-way ANOVA followed by post-hoc Tukey's test). N=6-7, data are representative of two individual cohorts of mice. (**B-F**) IRE1α-floxed mice were injected with Ad-Cre ($IRE1^{LKO}$), Ad-Cre together with Ad-IRE1 (IRE1-WT), or with Ad-Cre together with IRE1 SNO mutants (IRE1-M1+2)**.** N=4-6, data are representative of two individual cohorts of mice. UPR gene (**B**) UPR and RIDD gene expression (**C**) was examined in livers using quantitative real time PCR. **D**. Western blot analysis for the UPR status in the livers from these mice, with densitometric analysis shown in (**E**). Asterisk indicates statistical significance compared with control, and # indicates statistically significant differences between treatments (one-way ANOVA followed by post-hoc Tukey's test). IRE1α oligomerization in the livers of these mice. All data are shown as mean±S.E.M.

References:

1. D. Ron, P. Walter, Signal integration in the endoplasmic reticulum unfolded protein response. *Nat Rev Mol Cell Biol* **8**, 519-529 (2007).
2. G. S. Hotamisligil, Endoplasmic reticulum stress and the inflammatory basis of metabolic disease. *Cell* **140**, 900-917 (2010).
3. J. H. Lin, H. Li, D. Yasumura, H. R. Cohen, C. Zhang, B. Panning, K. M. Shokat, M. M. Lavail, P. Walter, IRE1 signaling affects cell fate during the unfolded protein response. *Science* **318**, 944-949 (2007).
4. Y. Wang, L. Vera, W. H. Fischer, M. Montminy, The CREB coactivator CRTC2 links hepatic ER stress and fasting gluconeogenesis. *Nature* **460**, 534-537 (2009).
5. F. Engin, A. Yermalovich, T. Nguyen, S. Hummasti, W. Fu, D. L. Eizirik, D. Mathis, G. S. Hotamisligil, Restoration of the unfolded protein response in pancreatic beta cells protects mice against type 1 diabetes. *Sci Transl Med* **5**, 211ra156 (2013).
6. C. Sidrauski, P. Walter, The transmembrane kinase Ire1p is a site-specific endonuclease that initiates mRNA splicing in the unfolded protein response. *Cell* **90**, 1031-1039 (1997).
7. A. H. Lee, N. N. Iwakoshi, L. H. Glimcher, XBP-1 regulates a subset of endoplasmic reticulum resident chaperone genes in the unfolded protein response. *Mol Cell Biol* **23**, 7448-7459 (2003).
8. U. Ozcan, Q. Cao, E. Yilmaz, A. H. Lee, N. N. Iwakoshi, E. Ozdelen, G. Tuncman, C. Gorgun, L. H. Glimcher, G. S. Hotamisligil, Endoplasmic reticulum stress links obesity, insulin action, and type 2 diabetes. *Science* **306**, 457-461 (2004).
9. N. Sreejayan, F. Dong, M. R. Kandadi, X. Yang, J. Ren, Chromium alleviates glucose intolerance, insulin resistance, and hepatic ER stress in obese mice. *Obesity* **16**, 1331-1337 (2008).
10. T. Mao, M. Shao, Y. Qiu, J. Huang, Y. Zhang, B. Song, Q. Wang, L. Jiang, Y. Liu, J. D. Han, P. Cao, J. Li, X. Gao, L. Rui, L. Qi, W. Li, Y. Liu, PKA phosphorylation couples hepatic inositol-requiring enzyme 1alpha to glucagon signaling in glucose metabolism. *Proc Natl Acad Sci USA* **108**, 15852-15857 (2011).
11. T. Nakamura, M. Furuhashi, P. Li, H. Cao, G. Tuncman, N. Sonenberg, C. Z. Gorgun, G. S. Hotamisligil, Double-stranded RNA-dependent protein kinase links pathogen sensing with stress and metabolic homeostasis. *Cell* **140**, 338-348 (2010).
12. X. Zhang, G. Zhang, H. Zhang, M. Karin, H. Bai, D. Cai, Hypothalamic IKKbeta/NF-kappaB and ER stress link overnutrition to energy imbalance and obesity. *Cell* **135**, 61-73 (2008).
13. C. N. Lumeng, A. R. Saltiel, Inflammatory links between obesity and metabolic disease. *J Clin Invest* **121**, 2111-2117 (2011).
14. M. F. Gregor, G. S. Hotamisligil, Inflammatory mechanisms in obesity. *Ann Rev Immunol* **29**, 415-445 (2011).
15. M. Kaneki, N. Shimizu, D. Yamada, K. Chang, Nitrosative stress and pathogenesis of insulin resistance. *Antioxid Redox Signal* **9**, 319-329 (2007).
16. B. T. Noronha, J. M. Li, S. B. Wheatcroft, A. M. Shah, M. T. Kearney, Inducible nitric oxide synthase has divergent effects on vascular and metabolic function in obesity. *Diabetes* **54**, 1082-1089 (2005).
17. M. Perreault, A. Marette, Targeted disruption of inducible nitric oxide synthase protects against obesity-linked insulin resistance in muscle. *Nat Med* **7**, 1138-1143 (2001).
18. T. Uehara, T. Nakamura, D. Yao, Z. Q. Shi, Z. Gu, Y. Ma, E. Masliah, Y. Nomura, S. A. Lipton, S-nitrosylated protein-disulphide isomerase links protein misfolding to neurodegeneration. *Nature* **441**, 513-517 (2006).
19. B. Derakhshan, P. C. Wille, S. S. Gross, Unbiased identification of cysteine S-nitrosylation sites on proteins. *Nat Protoc* **2**, 1685-1691 (2007).
20. S. R. Jaffrey, S. H. Snyder, The biotin switch method for the detection of S-nitrosylated proteins. *Sci STKE* **2001**, pl1 (2001).
21. D. T. Hess, A. Matsumoto, S. O. Kim, H. E. Marshall, J. S. Stamler, Protein S-nitrosylation: purview and parameters. *Nat Rev Mol Cell Biol* **6**, 150-166 (2005).
22. C. I. Murray, H. Uhrigshardt, R. N. O'Meally, R. N. Cole, J. E. Van Eyk, Identification and quantification of S-nitrosylation by cysteine reactive tandem mass tag switch assay. *Mol Cell Proteomics* **11**, M111 013441 (2012).

23. M. A. Carvalho-Filho, M. Ueno, S. M. Hirabara, A. B. Seabra, J. B. Carvalheira, M. G. de Oliveira, L. A. Velloso, R. Curi, M. J. Saad, S-nitrosation of the insulin receptor, insulin receptor substrate 1, and protein kinase B/Akt: a novel mechanism of insulin resistance. *Diabetes* **54**, 959-967 (2005).
24. T. Iwawaki, R. Akai, K. Kohno, IRE1alpha disruption causes histological abnormality of exocrine tissues, increase of blood glucose level, and decrease of serum immunoglobulin level. *PLoS One* **5**, e13052 (2010).
25. M. R. Talipov, Q. K. Timerghazin, Protein control of S-nitrosothiol reactivity: interplay of antagonistic resonance structures. *J Phys Chem B* **117**, 1827-1837 (2013).
26. K. P. Lee, M. Dey, D. Neculai, C. Cao, T. E. Dever, F. Sicheri, Structure of the dual enzyme Ire1 reveals the basis for catalysis and regulation in nonconventional RNA splicing. *Cell* **132**, 89-100 (2008).
27. R. L. Wiseman, Y. Zhang, K. P. Lee, H. P. Harding, C. M. Haynes, J. Price, F. Sicheri, D. Ron, Flavonol activation defines an unanticipated ligand-binding site in the kinase-RNase domain of IRE1. *Mol Cell* **38**, 291-304 (2010).
28. J. Hollien, J. H. Lin, H. Li, N. Stevens, P. Walter, J. S. Weissman, Regulated Ire1-dependent decay of messenger RNAs in mammalian cells. *J Cell Biol* **186**, 323-331 (2009).
29. M. Maurel, E. Chevet, J. Tavernier, S. Gerlo, Getting RIDD of RNA: IRE1 in cell fate regulation. *Trends Biochem Sci* **39**, 245-254 (2014).
30. Z. Wang, J. Tollervey, M. Briese, D. Turner, J. Ule, CLIP: construction of cDNA libraries for high-throughput sequencing from RNAs cross-linked to proteins in vivo. *Methods* **48**, 287-293 (2009).
31. J. M. Pagano, C. C. Clingman, S. P. Ryder, Quantitative approaches to monitor protein-nucleic acid interactions using fluorescent probes. *RNA* **17**, 14-20 (2011).
32. A. V. Korennykh, A. A. Korostelev, P. F. Egea, J. Finer-Moore, R. M. Stroud, C. Zhang, K. M. Shokat, P. Walter, Structural and functional basis for RNA cleavage by Ire1. *BMC biology* **9**, 47 (2011).
33. Y. Han, J. Donovan, S. Rath, G. Whitney, A. Chitrakar, A. Korennykh, Structure of human RNase L reveals the basis for regulated RNA decay in the IFN response. *Science* **343**, 1244-1248 (2014).
34. A. V. Korennykh, P. F. Egea, A. A. Korostelev, J. Finer-Moore, C. Zhang, K. M. Shokat, R. M. Stroud, P. Walter, The unfolded protein response signals through high-order assembly of Ire1. *Nature* **457**, 687-693 (2009).
35. R. Ghosh, L. Wang, E. Wang, B.G. Perera, A. Igbaria, S. Morita, K. Prado, M. Thamsen, D. Caswell, H. Macias, K.F. Weiberth, M.J. Gliedt, M.V. Alavi, S.B. Hari, A.K. Mitra, B. Bhhatarai, S. C. Schürer, E. L. Snapp, D.B. Gould, M.S. German, B.J. Backes, D.J. Maly, S.A. Oakes, F.R. Papa, Allosteric inhibition of the IRE1α RNase preserves cell viability and function during endoplasmic reticulum stress. *Cell* **158**, 534–548 (2014).
36. D. Han, A. G. Lerner, L. Vande Walle, J. P. Upton, W. Xu, A. Hagen, B. J. Backes, S. A. Oakes, F. R. Papa, IRE1alpha kinase activation modes control alternate endoribonuclease outputs to determine divergent cell fates. *Cell* **138**, 562-575 (2009).
37. A. Martinez-Ruiz, S. Lamas, Signalling by NO-induced protein S-nitrosylation and S-glutathionylation: convergences and divergences. *Cardiovasc Res* **75**, 220-228 (2007).
38. C. Hetz, The unfolded protein response: controlling cell fate decisions under ER stress and beyond. *Nat Rev Mol Cell Biol* **13**, 89-102 (2012).
39. S. W. Park, Y. Zhou, J. Lee, A. Lu, C. Sun, J. Chung, K. Ueki, U. Ozcan, The regulatory subunits of PI3K, p85alpha and p85beta, interact with XBP-1 and increase its nuclear translocation. *Nat Med* **16**, 429-437 (2010).
40. J. N. Winnay, J. Boucher, M. A. Mori, K. Ueki, C. R. Kahn, A regulatory subunit of phosphoinositide 3-kinase increases the nuclear accumulation of X-box-binding protein-1 to modulate the unfolded protein resposne. *Nat Med* **16**, 438-445 (2010).
41. F. Prischi, P. R. Nowak, M. Carrara, M. M. Ali, Phosphoregulation of Ire1 RNase splicing activity. *Nature Comm* **5**, 3554 (2014).
42. L. Wang, B. G. Perera, S. B. Hari, B. Bhhatarai, B. J. Backes, M. A. Seeliger, S. C. Schurer, S. A. Oakes, F. R. Papa, D. J. Maly, Divergent allosteric control of the IRE1alpha endoribonuclease using kinase inhibitors. *Nat Chem Biol* **8**, 982-989 (2012).

43. F. Urano, X. Wang, A. Bertolotti, Y. Zhang, P. Chung, H. P. Harding, D. Ron, Coupling of stress in the ER to activation of JNK protein kinases by transmembrane protein kinase IRE1. *Science* **287**, 664-666 (2000).
44. J. Hirosumi, G. Tuncman, L. Chang, C. Z. Gorgun, K. T. Uysal, K. Maeda, M. Karin, G. S. Hotamisligil, A central role for JNK in obesity and insulin resistance. *Nature* **420**, 333-336 (2002).
45. A. P. Arruda, B. M. Pers, G. Parlakgul, E. Guney, K. Inouye, G. S. Hotamisligil, Chronic enrichment of endoplasmic reticulum-mitochondria contact leads to mitochondrial dysfunction in obesity. *Nat Med* **20**, 1427-1435 (2014).
46. J. D. Horton, Y. Bashmakov, I. Shimomura, H. Shimano, Regulation of sterol regulatory element binding proteins in livers of fasted and refed mice. *Proc Natl Acad Sci U S A* **95**, 5987-5992 (1998).
47. H. Cao, K. Gerhold, J. R. Mayers, M. M. Wiest, S. M. Watkins, G. S. Hotamisligil, Identification of a lipokine, a lipid hormone linking adipose tissue to systemic metabolism. *Cell* **134**, 933-944 (2008).
48. M. Furuhashi, G. Tuncman, C. Z. Gorgun, L. Makowski, G. Atsumi, E. Vaillancourt, K. Kono, V. R. Babaev, S. Fazio, M. F. Linton, R. Sulsky, J. A. Robl, R. A. Parker, G. S. Hotamisligil, Treatment of diabetes and atherosclerosis by inhibiting fatty-acid-binding protein aP2. *Nature* **447**, 959-965 (2007).
49. F. Lisbona, D. Rojas-Rivera, P. Thielen, S. Zamorano, D. Todd, F. Martinon, A. Glavic, C. Kress, J. H. Lin, P. Walter, J. C. Reed, L. H. Glimcher, C. Hetz, BAX inhibitor-1 is a negative regulator of the ER stress sensor IRE1alpha. *Mol Cell* **33**, 679-691 (2009).
50. H. M. Berman, J. Westbrook, Z. Feng, G. Gilliland, T. N. Bhat, H. Weissig, I. N. Shindyalov, P. E. Bourne, The Protein Data Bank. *Nucleic Acids Research* **28**, 235-242 (2000).
51. D. Itzhak, M. Bright, P. McAndrew, A. Mirza, Y. Newbatt, J. Strover, M. Widya, A. Thompson, G. Morgan, I. Collins, F. Davies, Multiple autophosphorylations significantly enhance the endoribonuclease activity of human inositol requiring enzyme 1alpha. *BMC Biochem* **15**, 3 (2014).
52. T. Aviv, Z. Lin, S. Lau, L. M. Rendl, F. Sicheri, C. A. Smibert, The RNA-binding SAM domain of Smaug defines a new family of post-transcriptional regulators. *Nat Struct Biol* **10**, 614-621 (2003).
53. Y. Wang, T. Liu, C. Wu, H. Li, A strategy for direct identification of protein S-nitrosylation sites by quadrupole time-of-flight mass spectrometry. *J Am Soc Mass Spectrom* **19**, 1353-1360 (2008).